Degradation of FBXO31 by APC/C is regulated by AKT- and ATM-mediated phosphorylation

Srinadh Choppara[a,b,1], Sunil K. Malonia[c,d,1], Ganga Sankaran[a], Michael R. Green[c,d,2], and Manas Kumar Santra[a,2]

[a]Cancer Biology and Epigenetics Laboratory, National Centre for Cell Science, Ganeshkhind, 411 007 Pune, India; [b]Department of Biotechnology, Pune University, Ganeshkhind, 411 077 Pune, India; [c]Howard Hughes Medical Institute, University of Massachusetts Medical School, Worcester, MA 01605; and [d]Department of Molecular, Cell and Cancer Biology, University of Massachusetts Medical School, Worcester, MA 01605

Contributed by Michael R. Green, December 19, 2017 (sent for review April 10, 2017; reviewed by Sathees C. Raghavan and Susanta Roychoudhury)

The F-box protein FBXO31 is a tumor suppressor that is encoded in 16q24.3, for which there is loss of heterozygosity in various solid tumors. FBXO31 serves as the substrate-recognition component of the SKP/Cullin/F-box protein class of E3 ubiquitin ligases and has been shown to direct degradation of pivotal cell-cycle regulatory proteins including cyclin D1 and the p53 antagonist MDM2. FBXO31 levels are normally low but increase substantially following genotoxic stress through a mechanism that remains to be determined. Here we show that the low levels of FBXO31 are maintained through proteasomal degradation by anaphase-promoting complex/cyclosome (APC/C). We find that the APC/C coactivators CDH1 and CDC20 bind to a destruction-box (D-box) motif present in FBXO31 to promote its polyubiquitination and degradation in a cell-cycle–regulated manner, which requires phosphorylation of FBXO31 on serine-33 by the prosurvival kinase AKT. Following genotoxic stress, phosphorylation of FBXO31 on serine-278 by another kinase, the DNA damage kinase ATM, results in disruption of its interaction with CDH1 and CDC20, thereby preventing FBXO31 degradation. Collectively, our results reveal how alterations in FBXO31 phosphorylation, mediated by AKT and ATM, underlie physiological regulation of FBXO31 levels in unstressed and genotoxically stressed cells.

APC/C | FBXO31 | cell-cycle regulation | AKT | ATM

Anaphase-promoting complex/cyclosome (APC/C) is a large, multisubunit E3 ubiquitin ligase that regulates the progression through and exit from mitosis by polyubiquitinating cell-cycle regulators and targeting them for degradation by the 26S proteasome (1). APC/C substrates are recruited to the enzyme by interchangeable cell-cycle–regulated coactivator proteins. The two major APC/C coactivators are CDH1 and CDC20, which bind to their substrates at different times during the cell cycle and target them to APC/C, thus driving the cell cycle forward (2). CDC20 is active during mitosis and promotes anaphase onset by targeting mitotic cyclins and securin, whereas CDH1 becomes active during mitotic exit and has essential targets in the G1 phase (1, 3). The majority of CDH1 and CDC20 substrates contain a canonical destruction-box (D-box) motif, which is required for CDH1- and CDC20-dependent ubiquitination and degradation (2).

We have been studying the F-box protein FBXO31, a tumor suppressor encoded in 16q24.3, a region in which there is loss of heterozygosity in breast, ovarian, hepatocellular, and prostate cancers (4–8). FBXO31 serves as the substrate-recognition component of the SKP/Cullin/F-box protein class of E3 ubiquitin ligases (5). We initially identified FBXO31 as one of 17 factors required for oncogenic BRAF to induce senescence (9). We subsequently showed that, following genotoxic stress, FBXO31 is phosphorylated by the DNA damage kinase ataxia telangiectasia-mutated (ATM), resulting in increased levels of FBXO31, which can induce growth arrest in G1 or G2/M through two independent pathways that differ with regard to both substrates and p53 dependence (10, 11). In p53-positive cells following genotoxic stress, FBXO31 directly interacts with and mediates the degradation of MDM2, the major negative regulator of the tumor suppressor p53 (10). The decreased MDM2 results in increased levels of p53, which promote growth arrest and senescence through transcriptional activation of *p21* and other p53 target genes. In p53-deficient cells following genotoxic stress, FBXO31 interacts with and mediates degradation of cyclin D1, an important regulator of the G1/S transition, resulting in G1 arrest (11). FBXO31 has also been shown to target several other proteins, including the DNA replication factor CDT1 (12), the mitotic regulator FOXM1 (13), and the p38 activator MKK6 (14).

In unstressed cells, FBXO31 is maintained at a low level, resulting, at least in part, from proteasomal degradation (11). The mechanism by which FBXO31 is maintained at low levels in unstressed cells and is counteracted following DNA damage remains to be determined. Here we report that, in unstressed cells, FBXO31 levels are maintained at a low level by APC/C through the coordinated action of CDH1 and CDC20. We further show that APC/C-mediated degradation of FBXO31 is inhibited when FBXO31 is phosphorylated by ATM following genotoxic stress. Our results reveal the mechanism that regulates FBXO31 levels in unstressed cells and following genotoxic stress.

Results

FBXO31 Is Regulated Through Proteasomal Degradation Promoted by APC/C Coactivators CDH1 and CDC20. To begin studying the mechanism by which FBXO31 is maintained at low levels in unstressed cells, we first monitored endogenous FBXO31 expression throughout the cell cycle. Briefly, immortalized human embryonic kidney

Significance

The tumor suppressor protein FBXO31 is maintained at low levels in unstressed (normal cycling) cells, but rapidly increases following genotoxic stress (DNA damage), leading to induction of growth arrest or senescence. The mechanism that underlies physiological regulation of FBXO31 is unknown. Here we show that in unstressed cells FBXO31 is maintained at low levels by anaphase-promoting complex/cyclosome (APC/C), a ubiquitin ligase that targets cell-cycle regulatory substrates for proteasomal degradation. APC/C coactivators CDH1 and CDC20 interact with FBXO31 and coordinate its degradation, which requires phosphorylation by the prosurvival kinase AKT. Following genotoxic stress, FBXO31 is phosphorylated by another kinase, ATM, disrupting its interaction with CDH1 and CDC20 and preventing its degradation. Thus, altered phosphorylation underlies physiological regulation of FBXO31 levels.

Author contributions: S.C., S.K.M., M.R.G., and M.K.S. designed research; S.C., S.K.M., G.S., and M.K.S. performed research; S.K.M., M.R.G., and M.K.S. analyzed data; and S.K.M., M.R.G., and M.K.S. wrote the paper.

Reviewers: S.C.R., Indian Institute of Science; and S.R., Saroj Gupta Cancer Centre & Research Institute.

The authors declare no conflict of interest.

[1]S.C. and S.K.M. contributed equally to this work.

[2]To whom correspondence may be addressed. Email: michael.green@umassmed.edu or manas@nccs.res.in.

This article contains supporting information online at www.pnas.org/lookup/suppl/doi:10.1073/pnas.1705954115/-/DCSupplemental.

(HEK293T) cells were synchronized by treatment with the DNA replication inhibitor hydroxyurea (HU), which arrests cells at the G1/S boundary, and, following HU release, FBXO31 levels were detected by immunoblotting. As controls, we also monitored the cell-cycle–regulated proteins cyclin A and cyclin B. Consistent with previous reports (5, 12), we found that FBXO31 levels oscillated during the cell cycle: FBXO31 levels were low in late G1 to S, high in early G2 to G2/M, and then low from late M to G1 (Fig. 1*A* and Fig. S1*A*). *FBXO31* mRNA levels did not change during the cell cycle (Fig. S1*B*), confirming that cell-cycle regulation of FBXO31 occurred at the posttranscriptional level.

Notably, the cell-cycle–regulated pattern of FBXO31 protein levels showed similarity to those of cyclin B, which is degraded during mitotic exit and G1 by APC/C coactivators CDC20 and CDH1, respectively (15), suggesting that FBXO31 levels may be regulated by a similar mechanism. Consistent with this possibility, FBXO31 contains multiple D-box motifs (5), which, as stated above, reside in APC/C substrates targeted by CDH1 and CDC20. We therefore investigated the involvement of APC/C in regulating FBXO31. As a first test of this idea, we generated HEK293T cells stably expressing a control nonsilencing (NS) shRNA or an shRNA targeting APC2 or APC11, two catalytic subunits of APC/C (16), and monitored FBXO31 protein levels by immunoblotting. Knockdown of APC2 (Fig. 1*B*) or APC11 (Fig. S2*A*) resulted in increased FBXO31 protein levels compared with that obtained with a NS shRNA. Similar results were obtained with a second, unrelated APC2 or APC11 shRNA (Fig. 1*B* and Fig. S2*A*). Notably, knockdown of APC2 or APC11 resulted in a small increase in cells in G2/M (Fig. S2*B*), in which APC/C is known to be inactive (17), which likely contributes to the increased FBXO31 levels.

Next, we performed a series of experiments to determine whether FBXO31 levels were regulated by CDH1 and/or CDC20. First, we ectopically expressed CDH1 or CDC20 in HEK293T cells and monitored the levels of FBXO31, or as a control cyclin B, by immunoblotting. Ectopic expression of either CDH1 (Fig. 1*C*) or CDC20 (Fig. 1*D*) decreased levels of cyclin B, as expected, and also resulted in decreased levels of FBXO31. By contrast, ectopic expression of CDH1 or CDC20 failed to reduce FBXO31 levels in APC2-depleted cells (Fig. 1*E*). Addition of a proteasome inhibitor, MG132, blocked the ability of ectopically expressed CDH1 or CDC20 to decrease FBXO31 levels (Fig. 1 *C* and *D*), indicating that the CDH1- or CDC20-mediated decrease in FBXO31 resulted from proteasomal degradation. Consistent with this conclusion, *FBXO31* mRNA levels were unaffected by ectopic expression of CDH1 or CDC20 (Fig. S3*A*). Finally, we performed a cycloheximide chase/immunoblot assay and found that the half-life of endogenous FBXO31 was markedly reduced following ectopic expression of CDH1 or CDC20 (Fig. 1 *F* and *G* and Fig. S3 *B* and *C*).

We next performed a reciprocal set of experiments, in which we knocked down CDH1 or CDC20 and monitored FBXO31 levels. The immunoblots of Fig. 1 *H* and *I* show that shRNA-mediated knockdown of CDH1 or CDC20 in HEK293T cells resulted in increased FBXO31 protein levels. Consistent with these results, the half-life of endogenous FBXO31 was substantially longer in CDH1- or CDC20-depleted HEK293T cells than in NS shRNA-expressing cells (Fig. 1 *J* and *K* and Fig. S3 *D* and *E*). Similar results were obtained following knockdown of CDH1 or CDC20 in an unrelated cell line, MCF7 (Fig. S3 *F*–*I*). Collectively, these results demonstrate that APC/C regulates FBXO31 levels through CDH1 and CDC20.

The above experiments were performed in asynchronous cells, and we therefore sought to confirm the ability of CDH1 and CDC20 to regulate FBXO31 levels during specific phases of the cell cycle. Toward this end, we synchronized CDH1- or CDC20-depleted HEK293T cells with nocodazole, which arrests cells at the G2/M boundary. As controls, we monitored cyclin B and SKP2, which is targeted by CDH1 at G1 (18). Consistent with the results of Fig. 1*A*, in control cells expressing an NS shRNA, FBXO31 levels decreased following release from the G2/M transition (Fig. S4*A*). CDH1 knockdown resulted in increased FBXO31 levels predominantly from late M to G1. By contrast, CDC20 knockdown resulted in increased FBXO31 levels predominantly at late M. Knockdown of CDH1 or CDC20 resulted in a small increase in cells in G2/M (Fig. S4*B*), in which APC/C is known to be inactive (17), which likely contributes to the increased FBXO31 levels.

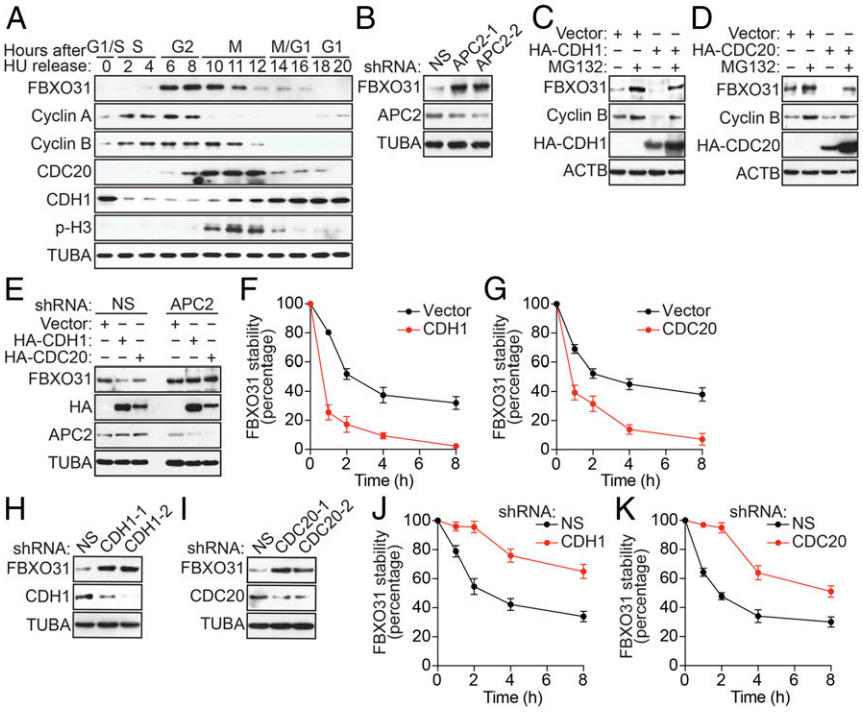

Fig. 1. FBXO31 is regulated through proteasomal degradation promoted by the APC/C coactivators CDH1 and CDC20. (*A*) Immunoblot monitoring FBXO31, cyclin A, cyclin B, CDH1, CDC20, and phospho-histone H3 (p-H3) in HEK293T cells following HU synchronization and release. p-H3 was used as a marker for mitotic cells. α-Tubulin (TUBA) was monitored as loading control. (*B*) Immunoblot analysis monitoring the levels of FBXO31 in HEK293T cells expressing a NS shRNA or one of two unrelated APC2 shRNAs. (*C* and *D*) Immunoblot monitoring FBXO31 and cyclin B levels in HEK293T cells expressing vector or HA-CDH1 (*C*) or HA-CDC20 (*D*) in the presence or absence of MG132. β-Actin (ACTB) was monitored as a loading control. (*E*) Immunoblot monitoring FBXO31 levels in HEK293T cells expressing vector, HA-CDH1, or HA-CDC20 and either a NS or a APC2 shRNA. (*F* and *G*) Quantification of cycloheximide chase/immunoblot assay monitoring FBXO31 stability in HEK293T cells expressing vector, HA-CDH1 (*F*), or HA-CDC20 (*G*). (*H* and *I*) Immunoblot monitoring FBXO31 levels in HEK293T cells expressing a NS shRNA or one of two unrelated CDH1 (*H*) or CDC20 (*I*) shRNAs. (*J* and *K*) Quantification of cycloheximide chase/immunoblot assay monitoring FBXO31 stability in HEK293T cells expressing a NS, CDH1 (*J*), or CDC20 (*K*) shRNA. Data are represented as mean ± SD.

Notably, *FBXO31* mRNA levels remained unchanged in CDH1- or CDC20-depleted cells following release from nocodazole arrest (Fig. S4*C*). Collectively, these results indicate that CDH1 and CDC20 promote degradation of FBXO31 during the G1 and late M phases of the cell cycle, respectively.

CDH1 and CDC20 Interact with FBXO31 Through Its First D-Box Motif, Which Is Required for Proteasomal Degradation. To test whether CDH1 and CDC20 interact with FBXO31, we performed a series of coimmunoprecipitation experiments. In all cases, HEK293T cells were pretreated with MG132 before preparation of protein extracts. Fig. 2 *A* and *B* shows that FBXO31 could be detected in CDH1 or CDC20 immunoprecipitates and, conversely, that CDH1 or CDC20 could be detected in the FBXO31 immunoprecipitates. Similar results were obtained in reciprocal coimmunoprecipitation experiments using ectopically expressed proteins (Fig. S5 *A* and *B*). To determine whether the interaction between FBXO31 and CDH1 or CDC20 occurred in a cell-cycle–dependent manner, HEK293T cells were synchronized using HU, and, following HU release, extracts from cells in G1/S, G2/M, or G1 phase were immunoprecipitated using an anti-CDH1 or anti-CDC20 antibody. As shown in Fig. 2*C*, FBXO31 interacted with CDH1 predominantly in the G1/S and G1 phases, whereas CDC20 interacted with FBXO31 in G2/M (Fig. S5*C*).

Both CDH1 and CDC20 interact with their substrates through a recognition motif known as a D-box, which consists of a simple core sequence of an arginine followed two residues later by a leucine (RxxL) (2, 19, 20). Analysis of the FBXO31 protein sequence revealed eight conserved putative D-box motifs (Fig. 2*D*). Previous studies with cyclin B have demonstrated that it contains two D-box motifs, the first of which is required to mediate protein degradation (21, 22). Therefore, as a first step toward delineating the functional D-box motif(s) in FBXO31, we generated an FBXO31 mutant in which residues 1–67, including the first D-box motif, were deleted [FBXO31(ΔD1)]. We ectopically coexpressed wild-type Flag-FBXO31 [FBXO31(WT)] or Flag-FBXO31(ΔD1) in the presence or absence of ectopically expressed CDH1 or CDC20 and monitored FBXO31 levels using an anti-Flag antibody. The immunoblots of Fig. 2 *E* and *F* demonstrate that the FBXO31(ΔD1) mutant was not degraded following ectopic expression of CDH1 or CDC20. The coimmunoprecipitation experiments of Fig. 2 *G* and *H* confirmed that, unlike FBXO31(WT), FBXO31(ΔD1) did not detectably interact with CDH1 or CDC20.

D-box–dependent substrate degradation can be ablated by mutating the arginine and leucine residues within the RxxL motif to alanine (22). To further substantiate the importance of the first D-box motif of FBXO31, we performed site-directed mutagenesis to generate a mutant in which both Arg-64 and Leu-67 were mutated to Ala (R64A/L67A). The immunoblots of Fig. 2 *I* and *J* show that the FBXO31(R64A/L67A) mutant was not degraded following ectopic expression of CDH1 or CDC20.

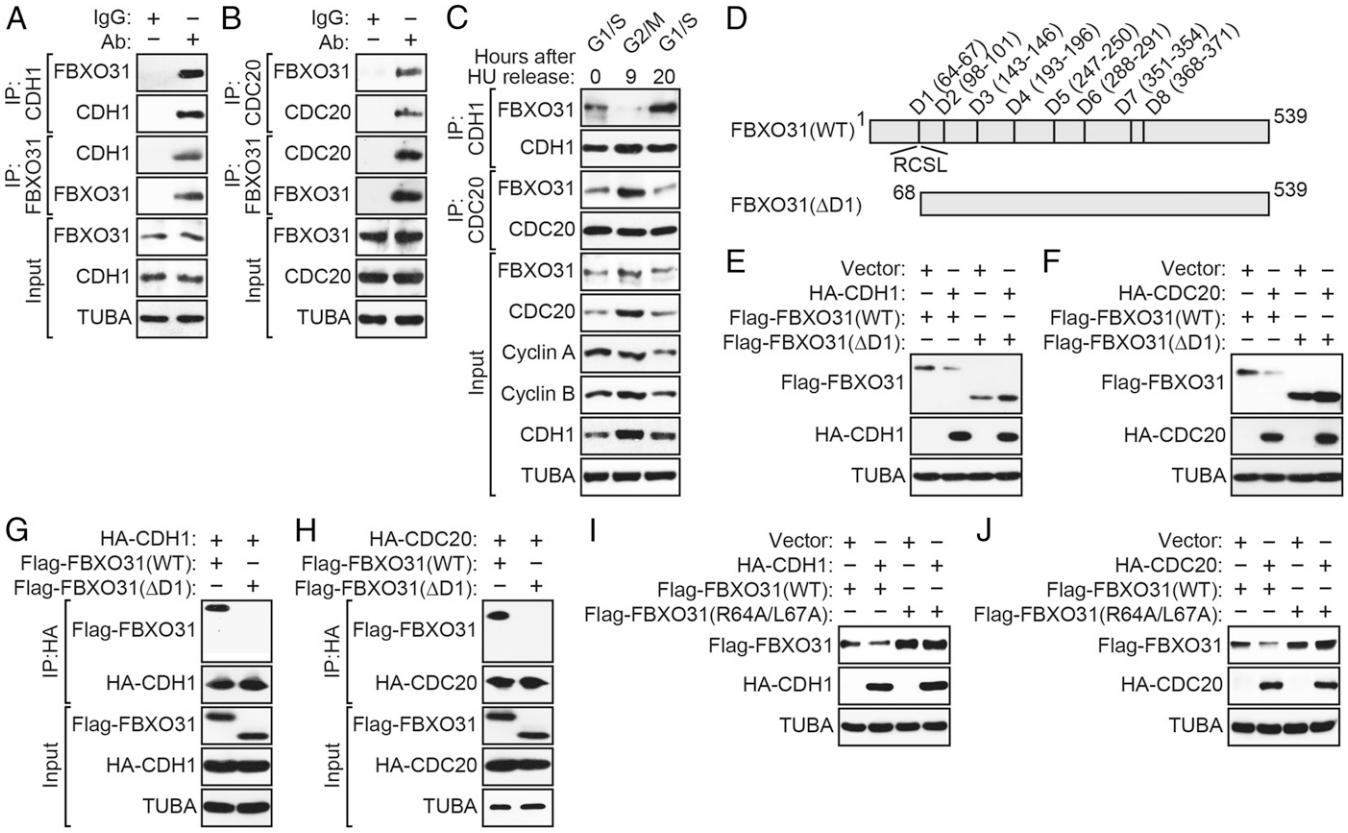

Fig. 2. CDH1 and CDC20 interact with FBXO31 through its first D-box motif, which is required for proteasomal degradation. (*A* and *B*) Coimmunoprecipitation monitoring the interaction between endogenous FBXO31 and CDH1 (*A*) or CDC20 (*B*) in asynchronous HEK293T cells. IgG was used as a nonspecific control. (*C*) Coimmunoprecipitation monitoring the interaction between endogenous FBXO31 and CDH1 or CDC20 in HU-synchronized HEK293T cells 0 h (G1/S), 9 h (G2/M), or 20 h (G1) after HU release. (*D*) Schematic of WT FBXO31 showing the positions of the eight D-boxes, as well as the FBXO31(ΔD1) and FBXO31(R64A,L67A) mutants. (*E* and *F*) Immunoblot monitoring Flag-FBXO31 levels (detected using an anti-Flag antibody) in HEK293T cells expressing Flag-FBXO31(WT) or Flag-FBXO31(ΔD1) and vector, HA-CDH1 (*E*), or HA-CDC20 (*F*). (*G* and *H*) Coimmunoprecipitation monitoring the interaction between ectopically expressed Flag-FBXO31(WT) or Flag-FBXO31(ΔD1) and HA-CDH1 (*G*) or HA-CDC20 (*H*) in HEK293T cells. (*I* and *J*) Immunoblot monitoring Flag-FBXO31 levels in HEK293T cells expressing Flag-FBXO31(WT) or Flag-FBXO31(R64A/L67A), and vector, HA-CDH1 (*I*), or HA-CDC20 (*J*).

Furthermore, the half-life of the FBXO31(R64A/L67A) mutant was substantially increased compared with FBXO31(WT) in cells ectopically expressing either CDH1 or CDC20 (Fig. S5 *D* and *E*). Collectively, these results indicate that the first D-box motif of FBXO31 is necessary for interaction with CDH1 and CDC20 and for subsequent degradation.

Polyubiquitination of FBXO31 by CDH1 or CDC20 Is Dependent on Phosphorylation by AKT Kinase. CDH1 and CDC20 interact with and promote polyubiquitylation of their substrates (23, 24). We therefore assessed whether CDH1 and CDC20 could promote polyubiquitination of FBXO31. In the first experiment, we performed an in vivo ubiquitination assay in which HEK293T cells were cotransfected with plasmids expressing His-ubiquitin, HA-CDH1, or HA-CDC20 and Flag-FBXO31(WT), Flag-FBXO31(ΔD1), or Flag-FBXO31(R64A/L67A). His-ubiquitin–conjugated proteins were purified using nickel beads under stringent denaturing conditions, followed by immunoblotting with an anti-Flag antibody. The results confirmed that ectopic expression of CDH1 (Fig. 3*A* and Fig. S6*A*) or CDC20 (Fig. 3*B* and Fig. S6*B*) promoted polyubiquitination of FBXO31(WT), but not of the FBXO31(ΔD1) or FBXO31(R64A/L67A) mutant.

Generally, recognition by E3 ubiquitin ligases requires phosphorylation of the substrate, which serves as a signal for ubiquitin-dependent destruction (25–27). Previous studies have shown that AKT has a prominent role in promoting progression through the cell cycle by acting on diverse downstream factors involved in controlling the G1/S and G2/M transitions (reviewed in ref. 28). We therefore hypothesized that AKT could mediate the phosphorylation of FBXO31 required for its degradation by APC/C. To determine whether AKT was involved in regulating FBXO31 stability, we expressed an shRNA targeting AKT in HEK293T cells and monitored FBXO31 levels by immunoblot analysis. Fig. 3*C* shows that shRNA-mediated knockdown of AKT led to increased FBXO31 levels. Consistent with this result, treatment of HEK293T cells with a specific AKT chemical inhibitor resulted in increased FBXO31 protein levels in a dose-dependent manner (Fig. 3*D*). We also observed that, following ectopic expression of CDH1 or CDC20, degradation of endogenous FBXO31 was decreased by the AKT inhibitor (Fig. 3 *E* and *F*). Likewise, polyubiquitination of endogenous FBXO31 was also significantly reduced by the AKT inhibitor (Fig. S7*A*).

Although we could not find a consensus AKT phosphorylation site in FBXO31, previous reports have demonstrated that AKT

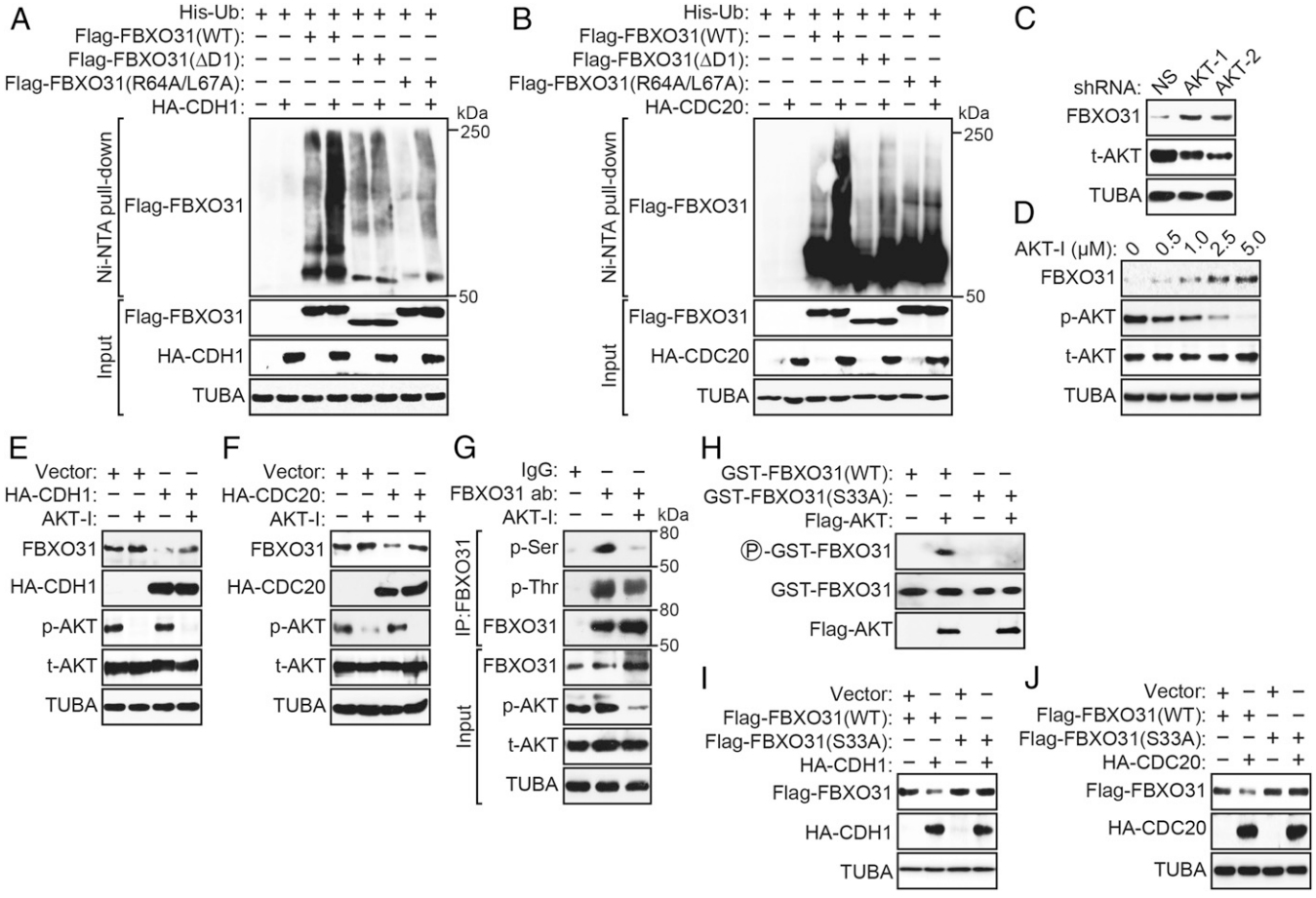

Fig. 3. Polyubiquitination of FBXO31 by CDH1 or CDC20 is dependent on phosphorylation by AKT kinase. (*A* and *B*) In vivo ubiquitination assay. HEK293T cells were cotransfected with plasmids expressing His-ubiquitin, Flag-FBXO31(WT), Flag-FBXO31(ΔD1), or Flag-FBXO31(R64A/L67A) and HA-CDH1 (*A*) or HA-CDC20 (*B*). Proteins bound to His-ubiquitin were purified by Ni-NTA pull-down, washed, and eluted in imidazole. Ubiquitinated Flag-FBXO31 was detected using an anti-Flag antibody. (*C*) Immunoblot monitoring the levels of FBXO31 and total AKT (t-AKT) in HEK293T cells expressing a NS shRNA or one of two unrelated AKT shRNAs. (*D*) Immunoblot monitoring FBXO31, phosphorylated AKT (p-AKT), and t-AKT in HEK293T cells treated with various concentrations of AKT inhibitor (AKT-I). (*E* and *F*) Immunoblot monitoring endogenous FBXO31 in HEK293T cells expressing HA-CDH1 (*E*) or HA-CDC20 (*F*) in the presence or the absence of AKT-I. (*G*) Coimmunoprecipitation monitoring the presence of phosphorylated Ser (p-Ser) or phosphorylated Thr (p-Thr) in the FBXO31 immunoprecipitate from HEK293T cells treated in the presence or the absence of AKT-I. (*H*) In vitro kinase assay monitoring the ability of purified AKT to phosphorylate GST-FBXO31(WT) or GST-FBXO31(S33A). (*I* and *J*) Immunoblot monitoring levels of Flag-FBXO31(WT) or Flag-FBXO31(S33A) in HEK293T cells expressing vector, HA-CDH1 (*I*), or HA-CDC20 (*J*).

can phosphorylate substrates independent of the consensus sequence (29, 30). As a first step to determine which residue of FBXO31 was phosphorylated by AKT, we immunoprecipitated FBXO31 in the presence or absence of AKT inhibitor followed by immunoblotting with an anti–phosphorylated-Ser (p-Ser) or anti–phosphorylated-Thr (p-Thr) antibody to detect phosphorylated residues. The results of Fig. 3*G* show that the p-Ser signal in the FBXO31 immunoprecipitate was abrogated by treatment with the AKT inhibitor, whereas the p-Thr signal was only modestly affected. To predict which specific serine residue(s) of FBXO31 are likely to be phosphorylated by AKT, we queried the PhosphoSite database (31), which revealed Ser-33 as the most highly reported phosphorylated residue in FBXO31. To determine whether AKT phosphorylates FBXO31 at Ser-33, we constructed an FBXO31 derivative in which Ser-33 was mutated to Ala [FBXO31(S33A)]. The in vitro kinase assay of Fig. 3*H* shows that AKT could phosphorylate FBXO31(WT) but not FBXO31(S33A), demonstrating that AKT directly phosphorylates FBXO31 at Ser-33.

Next, we tested the ability of CDH1 and CDC20 to degrade the phosphorylation-defective FBXO31(S33A) mutant. Immunoblot analysis showed that FBXO31(S33A) was not degraded following ectopic expression of CDH1 (Fig. 3*I*) or CDC20 (Fig. 3*J*). Furthermore, an in vivo ubiquitination assay showed that, unlike FBXO31(WT), ectopically expressed CDH1 or CDC20 failed to promote polyubiquitination of FBXO31(S33A) (Fig. S7*B*).

Finally, we confirmed these in vivo results using an in vitro ubiquitination assay. In brief, we assembled reaction mixtures containing FBXO31 and cofactors (E1, E2, ubiquitin, and ATP) in the presence or absence of AKT and either CDH1 or CDC20 immunopurified from transfected HEK293T cells (i.e., associated with APC/C). Fig. S7*C* shows that immunopurified CDH1 or CDC20 promoted polyubiquitination of FBXO31 in vitro in the presence but not the absence of AKT. Collectively, these results show that polyubiquitination of FBXO31 directed by CDH1 or CDC20 and subsequent degradation is dependent upon phosphorylation of FBXO31 by AKT.

Interaction Between FBXO31 and CDH1 or CDC20 Is Perturbed Following DNA Damage. Previous studies have shown that diverse DNA-damaging agents increase FBXO31 levels, indicating that stabilization of FBXO31 is a general response to genotoxic stress (11, 14). We therefore sought to determine whether the stabilization of FBXO31 following DNA damage is due to the loss of interaction with CDH1 and CDC20. To test this idea, we performed coimmunoprecipitation experiments in HEK293T cells that were either untreated or treated with a DNA-damaging agent. Following treatment with ionizing radiation (IR) (Fig. 4*A*) or the topoisomerase inhibitor doxorubicin (Fig. S8*A*), the interaction between endogenous FBXO31 and CDH1 or CDC20 was lost. Similar results were obtained following treatment of MCF7 cells with either IR or the topoisomerase inhibitor etoposide (Fig. S8 *B* and *C*).

Our previous study showed that DNA-damage–induced stabilization of FBXO31 is mediated posttranslationally by ATM, which phosphorylates FBXO31 at Ser-278/Gln-279 (11). To determine whether the loss of the FBXO31–CDH1 or FBXO31–CDC20 interaction following DNA damage was due to phosphorylation of FBXO31 by ATM, we performed coimmunoprecipitation experiments in irradiated HEK293T cells following shRNA-mediated depletion of ATM. As shown in Fig. 4*B*, CDH1 and CDC20 failed to interact with FBXO31 in irradiated cells expressing a control NS shRNA. However, in ATM-depleted cells, the interaction of FBXO31 with CDH1 or CDC20 still occurred following irradiation. By contrast, in cells depleted of the catalytic subunit of another DNA damage kinase, DNA-dependent protein kinase (DNA-PKcs), CDH1 and CDC20 failed to interact with FBXO31 in irradiated cells (Fig. S9*A*). Thus, loss of the FBXO31–CDH1 and FBXO31–CDC20 interactions is not a general consequence of activation of the DNA damage response. These results suggest that ATM-mediated phosphorylation of FBXO31 on Ser-278 prevents interaction between FBXO31 and CDH1 or CDC20, which leads to stabilization of FBXO31 following DNA damage.

Several previous reports have suggested that genotoxic stress inactivates AKT signaling (32–34), and we therefore sought to determine if AKT-mediated phosphorylation of FBXO31 was reduced following genotoxic stress. Toward this end, we generated an FBXO31 derivative containing residues 1–100 [FBXO31 (1–100)], which harbors the AKT phosphorylation site (Ser-33) but lacks the ATM phosphorylation site (Ser-278). We then monitored serine phosphorylation of the FBXO31(1–100) derivative following DNA damage by treatment of HEK293T cells with IR. We found that the FBXO31(1–100) derivative was phosphorylated in unstressed cells, as expected, and was unaffected following treatment with IR (Fig. S9*B*). Consistent with this result, we also found that in IR-treated cells, serine phosphorylation of FBXO31 was not increased following treatment with an ATM inhibitor, indicating that ATM-mediated phosphorylation of FBXO31 does not impede AKT-mediated phosphorylation (Fig. S9*C*). Collectively, these results indicate that AKT-mediated Ser-33 phosphorylation persists even following genotoxic stress.

Discussion

The results of our study are summarized in the model of Fig. 4*C*. In unstressed cells, FBXO31 levels are low due to proteasomal degradation mediated by the coordinated action of the APC/C coactivators CDH1 and CDC20. In these cells, FBXO31 is

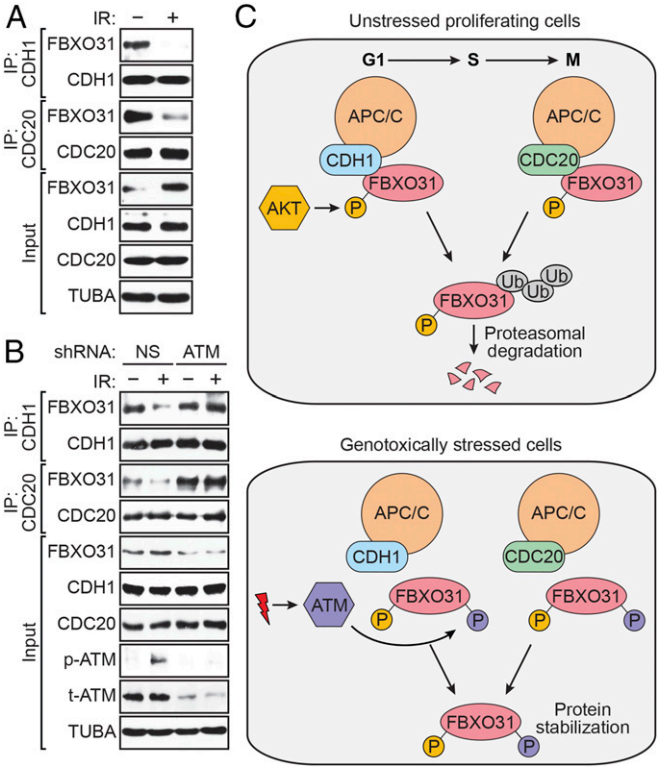

Fig. 4. Interaction between FBXO31 and CDH1 or CDC20 is perturbed following DNA damage. (*A*) Coimmunoprecipitation monitoring the interaction between endogenous FBXO31 and CDH1 or CDC20 in asynchronous HEK293T cells treated with or without IR. (*B*) Coimmunoprecipitation monitoring the interaction between endogenous FBXO31 and CDH1 or CDC20 in HEK293T cells expressing a NS or ATM shRNA, with or without IR. (*C*) Model for regulation of FBXO31 by APC/C.

phosphorylated at Ser-33 by AKT, a well-known proliferative protein kinase (35). Following genotoxic stress, FBXO31 is phosphorylated by the DNA damage kinase ATM, which results in loss of interaction with CDH1 and CDC20, leading to increased FBXO31 levels. Notably, AKT-mediated Ser-33 phosphorylation is not reduced following DNA damage (Fig. S9*B*). Therefore, ATM-mediated phosphorylation of Ser-278, even in the presence of Ser-33 phosphorylation, is sufficient to trigger loss of interaction with CDH1 and CDC20, leading to FBXO31 stabilization. Thus, our results reveal how alterations in FBXO31 phosphorylation, mediated by AKT and ATM, underlie physiological regulation of FBXO31 levels in unstressed and genotoxically stressed cells.

CDH1/CDC20-mediated regulation of FBXO31 occurs in a cell-cycle–dependent manner, with CDH1 targeting FBXO31 in G1 and CDC20 targeting FBXO31 in late M phase. By contrast, FBXO31 levels are elevated from early G2 to G2/M. Consistent with this result, two previous studies have provided evidence for FBXO31 playing key roles in early G2 to G2/M. First, in early-to-mid G2, FBXO31 targets the DNA replication licensing factor CDT1 to prevent rereplication (12). Second, FBXO31 plays an important role during the G2/M transition, where it regulates the levels of FOXM1, a transcription factor and master regulator of mitosis (13). Notably, FBXO31 levels are low in S phase, when APC/C is inactive; the mechanism(s) and factor(s) that regulate FBXO31 levels during S phase remain to be determined.

FBXO31 is a tumor suppressor that is stabilized in response to various genotoxic stresses (11, 14) and functions by maintaining genomic stability by activating cell-cycle checkpoints and inducing senescence or growth arrest (10, 11, 13) or protecting cells from stress-induced apoptosis (14). Collectively, our results reveal the mechanism required for physiologically regulating FBXO31 levels in unstressed cells and following genotoxic stress, which is essential to its tumor suppressor function.

Materials and Methods

Materials and methods used for cell culture, cell synchronization, drug treatment, plasmid construction (including mutagenesis), RNAi, qRT-PCR, immunoblotting and coimmunoprecipitation, cycloheximide chase, in vitro kinase assays, and in vitro and in vivo ubiquitination assays are available in *SI Materials and Methods*. All quantitative data were collected from experiments performed in at least triplicate and are expressed as mean ± SD or SEM.

ACKNOWLEDGMENTS. We thank the University of Massachusetts Medical School RNAi Core Facility for providing shRNAs and S. Deibler for editorial assistance. This work was supported in part by a Ramalingaswami Fellowship from the Department of Biotechnology, Government of India (to M.K.S.). M.R.G. is an investigator of the Howard Hughes Medical Institute.

1. Sivakumar S, Gorbsky GJ (2015) Spatiotemporal regulation of the anaphase-promoting complex in mitosis. *Nat Rev Mol Cell Biol* 16:82–94.
2. Pfleger CM, Lee E, Kirschner MW (2001) Substrate recognition by the Cdc20 and Cdh1 components of the anaphase-promoting complex. *Genes Dev* 15:2396–2407.
3. Manchado E, Eguren M, Malumbres M (2010) The anaphase-promoting complex/cyclosome (APC/C): Cell-cycle-dependent and -independent functions. *Biochem Soc Trans* 38:65–71.
4. Härkönen P, Kyllönen AP, Nordling S, Vihko P (2005) Loss of heterozygosity in chromosomal region 16q24.3 associated with progression of prostate cancer. *Prostate* 62:267–274.
5. Kumar R, et al. (2005) FBXO31 is the chromosome 16q24.3 senescence gene, a candidate breast tumor suppressor, and a component of an SCF complex. *Cancer Res* 65:11304–11313.
6. Launonen V, et al. (2000) Loss of heterozygosity at chromosomes 3, 6, 8, 11, 16, and 17 in ovarian cancer: Correlation to clinicopathological variables. *Cancer Genet Cytogenet* 122:49–54.
7. Lin YW, et al. (2001) Deletion mapping of chromosome 16q24 in hepatocellular carcinoma in Taiwan and mutational analysis of the 17-beta-HSD gene localized to the region. *Int J Cancer* 93:74–79.
8. Miller BJ, Wang D, Krahe R, Wright FA (2003) Pooled analysis of loss of heterozygosity in breast cancer: A genome scan provides comparative evidence for multiple tumor suppressors and identifies novel candidate regions. *Am J Hum Genet* 73:748–767.
9. Wajapeyee N, Serra RW, Zhu X, Mahalingam M, Green MR (2008) Oncogenic BRAF induces senescence and apoptosis through pathways mediated by the secreted protein IGFBP7. *Cell* 132:363–374.
10. Malonia SK, Dutta P, Santra MK, Green MR (2015) F-box protein FBXO31 directs degradation of MDM2 to facilitate p53-mediated growth arrest following genotoxic stress. *Proc Natl Acad Sci USA* 112:8632–8637.
11. Santra MK, Wajapeyee N, Green MR (2009) F-box protein FBXO31 mediates cyclin D1 degradation to induce G1 arrest after DNA damage. *Nature* 459:722–725.
12. Johansson P, et al. (2014) SCF-FBXO31 E3 ligase targets DNA replication factor Cdt1 for proteolysis in the G2 phase of cell cycle to prevent re-replication. *J Biol Chem* 289:18514–18525.
13. Jeffery JM, et al. (2016) FBXO31 protects against genomic instability by capping FOXM1 levels at the G2/M transition. *Oncogene* 36:1012–1022.
14. Liu J, et al. (2014) F-box only protein 31 (FBXO31) negatively regulates p38 mitogen-activated protein kinase (MAPK) signaling by mediating lysine 48-linked ubiquitination and degradation of mitogen-activated protein kinase kinase 6 (MKK6). *J Biol Chem* 289:21508–21518.
15. Raff JW, Jeffers K, Huang JY (2002) The roles of Fzy/Cdc20 and Fzr/Cdh1 in regulating the destruction of cyclin B in space and time. *J Cell Biol* 157:1139–1149.
16. Chang LF, Zhang Z, Yang J, McLaughlin SH, Barford D (2014) Molecular architecture and mechanism of the anaphase-promoting complex. *Nature* 513:388–393.
17. Peters JM (2006) The anaphase promoting complex/cyclosome: A machine designed to destroy. *Nat Rev Mol Cell Biol* 7:644–656.
18. Bashir T, Dorrello NV, Amador V, Guardavaccaro D, Pagano M (2004) Control of the SCF(Skp2-Cks1) ubiquitin ligase by the APC/C(Cdh1) ubiquitin ligase. *Nature* 428:190–193.
19. He J, et al. (2013) Insights into degron recognition by APC/C coactivators from the structure of an Acm1-Cdh1 complex. *Mol Cell* 50:649–660.
20. Pfleger CM, Kirschner MW (2000) The KEN box: An APC recognition signal distinct from the D box targeted by Cdh1. *Genes Dev* 14:655–665.
21. Glotzer M, Murray AW, Kirschner MW (1991) Cyclin is degraded by the ubiquitin pathway. *Nature* 349:132–138.
22. King RW, Glotzer M, Kirschner MW (1996) Mutagenic analysis of the destruction signal of mitotic cyclins and structural characterization of ubiquitinated intermediates. *Mol Biol Cell* 7:1343–1357.
23. Brown NG, et al. (2014) Mechanism of polyubiquitination by human anaphase-promoting complex: RING repurposing for ubiquitin chain assembly. *Mol Cell* 56:246–260.
24. Van Voorhis VA, Morgan DO (2014) Activation of the APC/C ubiquitin ligase by enhanced E2 efficiency. *Curr Biol* 24:1556–1562.
25. Badodi S, Baruffaldi F, Ganassi M, Battini R, Molinari S (2015) Phosphorylation-dependent degradation of MEF2C contributes to regulate G2/M transition. *Cell Cycle* 14:1517–1528.
26. Hellmuth S, Böttger F, Pan C, Mann M, Stemmann O (2014) PP2A delays APC/C-dependent degradation of separase-associated but not free securin. *EMBO J* 33:1134–1147.
27. Skowyra D, Craig KL, Tyers M, Elledge SJ, Harper JW (1997) F-box proteins are receptors that recruit phosphorylated substrates to the SCF ubiquitin-ligase complex. *Cell* 91:209–219.
28. Xu N, Lao Y, Zhang Y, Gillespie DA (2012) Akt: A double-edged sword in cell proliferation and genome stability. *J Oncol* 2012:951724.
29. Du K, Montminy M (1998) CREB is a regulatory target for the protein kinase Akt/PKB. *J Biol Chem* 273:32377–32379.
30. Sutherland BW, et al. (2005) Akt phosphorylates the Y-box binding protein 1 at Ser102 located in the cold shock domain and affects the anchorage-independent growth of breast cancer cells. *Oncogene* 24:4281–4292.
31. Hornbeck PV, et al. (2015) PhosphoSitePlus, 2014: Mutations, PTMs and recalibrations. *Nucleic Acids Res* 43:D512–D520.
32. Kandel ES, et al. (2002) Activation of Akt/protein kinase B overcomes a G(2)/m cell cycle checkpoint induced by DNA damage. *Mol Cell Biol* 22:7831–7841.
33. Mukherji A, Janbandhu VC, Kumar V (2009) HBx protein modulates PI3K/Akt pathway to overcome genotoxic stress-induced destabilization of cyclin D1 and arrest of cell cycle. *Indian J Biochem Biophys* 46:37–44.
34. Zundel W, Giaccia A (1998) Inhibition of the anti-apoptotic PI(3)K/Akt/Bad pathway by stress. *Genes Dev* 12:1941–1946.
35. Hers I, Vincent EE, Tavaré JM (2011) Akt signalling in health and disease. *Cell Signal* 23:1515–1527.
36. Benjamini Y, Hochberg Y (1995) Controlling the false discovery rate: A practical and powerful approach to multiple testing. *J R Stat Soc B* 57:289–300.